

**Target screening of the new compound JBIR-19 using
budding yeast gene-deletion mutants**

Hayato Ogawa

Department of Integrated Biosciences
Graduate School of Frontier Sciences
The University of Tokyo

2010

Master Thesis

Table of Contents

List of Figures	1
List of Tables	2
Acknowledgements	3
Abbreviations	4
Summary	5
Introduction	6
Results	10
Discussion	15
Materials and Methods	18
References	25
Figures.....	30
Tables	42

List of Figures

Figure 1. The structure of JBIR-19(A) and phase contrast image of diploid wild-type cells *S. cerevisiae* grown in the presence or absence of JBIR-19(B).

Figure 2. Deletion cassette used for constructing strains in the yeast deletion collection.

Figure 3. Outline of the competitive growth assay.

Figure 4. Possible explanation of results.

Figure 5. Growth inhibition by JBIR-19 for wild type strain.

Figure 6. Outline for experimental procedure.

Figure 7. The deletion strains specifically sensitive to JBIR-19 with a competitive growth assay.

Figure 8. Deletion mutant of *DHH1* showed sensitivity to JBIR-19 in a concentration-dependent manner.

Figure 9. Deletion mutant of *DHH1* showed sensitivity to bleomycin in a concentration-dependent manner.

Figure 10. JBIR-19 and bleomycin induced elongated bud morphology of wild-type cells and *Δdhh1* cells.

Figure 11. JBIR-19 induces the delay of *CLN2* mRNA accumulation in haploid *Δdhh1* cells.

Figure 12. The G1/S transition delay induced by JBIR-19 in *Δdhh1* cells.

List of Tables

Table 1. Combination of growth conditions and dyes for each array

Table 2. 50% inhibition concentration (IC₅₀) of bleomycin for wild-type strain and *Δdhh1*

Acknowledgements

I wish to express my deepest gratitude to an outstanding and experienced Geneticist, Prof. Yoshikazu Ohya for his supervision and advice through this study.

I thank Dr. Satoru Nogami for his helpful advice, discussion and encouragement.

I would also like to express my sincere gratitude to Takahiro Negishi, Mizuho Sekiya,, Shinsuke Ohnuki, and Yo Kikuchi for great help.

I would like to thank Seiko Morinaga for their technical support.

I would like to Dr. Kazuo Shinya providing JBIR-19 and collaborating for isolation and identification of compounds.

I also thank all members of the Laboratory of Signal Transduction, Department of Integrated Biosciences, Graduate School of Frontier Sciences, the University of Tokyo, for their encouragement.

I am grateful to Hiroki Okada, Tomohide Kobayashi, Tomoko Motohashi, Taku Mohri, and Keiichi Takeda for their mental supporting.

Last but not least, I also thank my family for mental and financial support.

Abbreviations

AIST	: National Institute of Advanced Industrial Science and Technology
DIG	: Digoxigenin
DMSO	: Dimethyl Sulfoxide
PCR	: polymelase chain reaction
SDS	: sodium dodecyl sulfate
Tris:	: Tris (hydroxymethyl) aminomethane

Summary

The identification of targets of bioactive compounds is an essential task for development of novel drugs because it can contribute to understand their cellular modes of action. However, it is difficult to identify the mode of action or the cellular target. A set of gene deletion mutants of *Saccharomyces cerevisiae* was constructed and has been a powerful tool to identify drug target. Here, using the gene-deletion set, I investigated the target of a novel compound JBIR-19, which was isolated from the cell morphology-based screening in *S. cerevisiae* (Kozone *et al.*, 2009). First, to elucidate the cellular mode of action of JBIR-19, gene-deletion strains, which show specific sensitivity to JBIR-19, were screened by competitive growth assay with 1133 heterozygous essential gene-deletion strains and 4548 homozygous non-essential gene-deletion strains. Seven gene-deletion strains reproducibly showed sensitivity to JBIR-19. The confirmation of this assay revealed that homozygous deletion of *DHH1* among these 7 strains was significantly sensitive to JBIR-19, and the sensitivity was in a concentration-dependent manner. In addition, JBIR-19 induced elongated bud morphology in homozygous $\Delta dhh1$ cells, suggesting that the effect of JBIR-19 is similar to DNA damaging agents. Finally, JBIR-19 induced the delay of G1/S cyclin *CLN2* mRNA accumulation in haploid $\Delta dhh1$ cells. These results strongly indicate that the cellular target of JBIR-19 is the product of a gene, of which deletion is synthetically lethal with *DHH1* deletion. The product is possibly required for bud formation and G1/S transition. These results provide the clues for identification of cellular target of JBIR-19 and to understand the cellular mechanism affected by JBIR-19.

Introduction

Since bioactive compounds can modulate protein function, they are widely used not only as therapeutic agents but also as valuable research tools (Parsons *et al.*, 2004). Especially, the activities and chemical structures of bioactive compounds from natural products are so diversified that they are thought to be a rich source of novel drugs. However, although many effective therapeutic agents in the market are derived from natural products, they are often administered without *a priori* knowledge of the target or underlying mechanism of action. Thus, identification of bioactive compounds' target is important to design new compounds with improved safety and efficacy profiles (Giaever *et al.*, 2003, Hoon *et al.*, 2008).

Identification of drug targets remains one of the most difficult and challenging tasks. Traditional approaches for target identification involve biochemical purification of the protein target. For instance, targets of immunosuppressants FK506 and cyclosporine A, the immunophilin and cyclophilin, respectively, were identified using small molecule affinity matrices and subsequent purification of their binding proteins from bovine thymus and human spleen (Harding *et al.*, 1989). However, methods such as these are often labor intensive and need to be tailored to individual proteins and compounds.

The ease of genetic manipulation, combined with its level of gene conservation with humans (40-50%), makes budding yeast *Saccharomyces cerevisiae* a powerful model organism to identify genes involved in drug responses. An attempt to isolate drug targets in yeast was first documented over 20 years ago (Rine *et al.*, 1983). In that study, the protein targets of two compounds, compactin and tunicamycin, were identified by

screening a genomic library for genes that confer drug-resistance when overexpressed. For comprehensive and systematic survey of genetic interactions in yeast, collections of yeast mutants have been constructed. Yeast deletion collections consists of -4,800 haploid deletion strains (*MATa* mating type), -4,800 haploid deletion strains (*MAT α* mating type), -4,800 diploid homozygous deletion strains, and -6,000 diploid heterozygous deletion strains of *S. cerevisiae*. Each mutant possess a precise deletion (from the start to the stop codon) in one of all 6,000 yeast genes (Winzeler *et al.*, 1999; Giaever, *et al.*, 2002). A method to detect growth rate of all *S. cerevisiae* gene-deletion strains under the certain conditions has recently been available. Thus, this collection of ‘6000 genes’ can be assayed to identify all genes that affect growth under the conditions in the presence of a compound.

Haploid and homozygote collections are useful to identify target molecules or pathways of a drug. Lee *et al.*, assayed the effects of 12 DNA-damaging agents on the complete pool of approximately 4,700 homozygous deletion strains in yeast (Lee *et al.*, 2005). These screens identified genes in well-characterized DNA-damage-response pathways as well as genes whose role in the DNA-damage response had not been previously established. Each compound produced a unique genome-wide profile. Clustering the profile data for 12 distinct compounds uncovered both known and novel functional interactions that comprise the DNA-damage response. The use of heterozygotes has also proven to be particularly powerful for drug target-identification *in vivo*. The analysis with 233 yeast heterozygous deletions of drug target genes was firstly applied to monitor compound activities *in vivo* and identified the known target and two hyper sensitive loci in a mixed culture of 233 strains in the presence of the drug tunicamycin (Giaever *et al.*, 1999). This anaysis showed that reducing the copy number

of a gene which codes drug target from two to one in a diploid cell can result in sensitization to the drug of interest. This point of view was used to identify the known targets of a few well-characterized compounds using competitive growth experiments with small pools of heterozygous deletion mutants. Extending this approach to larger strain pools and diverse compound libraries to identify novel drug targets, a pool of nearly 4,000 heterozygots was tested against 78 diverse chemical treatments (Lum, *et al.*, 2004). In this study, specifically, lanosterol synthase in the sterol biosynthetic pathway was identified as a target of the antianginal drug molsidomine, which may explain its cholesterol-lowering effects and the rRNA processing exosome was identified as a potential target of the cell growth inhibitor 5-fluorouracil. These comprehensive and efficient approaches enable to identify known or novel protein targets and pathways of bioactive compounds..

Recently, Kozone *et al.*, carried out the chemical screening focusing on a specific morphology of *S.cerevisiae* (Kozone *et al.*,2009). Because cell morphology in *S.cerevisiae* is tightly linked to cellular processes and functions (Ohya, *et al.*, 2005, Watanabe, *et al.*, 2009), morphology-based screening is thought to aim at a specific cellular process or function. They performed the screen of the compounds inducing abnormal morphology. In that screen, a novel compound JBIR-19 was isolated from the culture broth of an entomopathogenic fungus *Metarhizium* sp. fE61V. Its structure was determined to be 24-membered macrolide analogs on the basis of NMR and other spectroscopic data (Figure 1A). This compound induced striking elongated morphology of *S.cerevisiae* (Figure 1B), and showed weak anti-yeast activity at minimum inhibition concentration of 200 μ M.

In this study, I attempted to identify the target of a novel compound JBIR-19 to

find out its mode of action. Mutants showing a JBIR-19-specific growth defect were screened from 1133 heterozygous essential gene-deletion mutants and 4548 homozygous non-essential gene-deletion mutants. The deletion of *DHH1*, a non-essential gene, was specifically sensitive to JBIR-19. Furthermore, in $\Delta dhh1$ cells, JBIR-19 induced elongated bud morphology and the delay of G1/S transition. These results give hint to elucidate the cellular mode of action of JBIR-19.

Results

Screening of mutants specifically sensitive to JBIR-19

To elucidate mode of action of JBIR-19 in yeast, mutants showing JBIR-19-specific growth defect were screened from 1133 heterozygous essential gene deletion strains and 4548 homozygous non-essential gene deletion strains. A method has recently established to detect growth rate of all *S. cerevisiae* gene-deletion strains each of which is uniquely tagged with 20 base barcode DNA (Figure 2) in the presence of a compound. This method allows fitness to be measured by tracking changes in strain abundance using a microarray carrying the complements of the tag sequences (Figure 3, Pierce *et al.*, 2007). I performed this competitive growth assay to identify gene-deletion strains specific sensitivity to JBIR-19.

First, I determined the concentration of JBIR-19 to treat for the competitive growth assay. The gene-deletion strain pooled culture is grown competitively with or without the presence of treatment. The concentration of treatment should be 10-20% decrease in growth rate for the wild-type strain (Pierce, *et al.*, 2007). This percentage decrease in growth is a standard common level of inhibition to simplify the experimental setup (Pierce, *et al.*, 2007). Standardizing the level of inhibition allows most experiments to be sampled after the same number of generations. To determine the concentration of JBIR-19 to grow the gene-deletion strain pooled culture, wild-type diploid strain (BY4743) was grown in the presence of various concentrations of JBIR-19 and cell growth were monitored with optical density at 600

nm (Figure 5A). The relative growth inhibition rate was calculated with as a ratio of the doubling time in growth with JBIR-19 to that or without JBIR-19. As shown Figure 5B, growth inhibition ratio rates of at 2.5 and 5 μ M JBIR-19 was were between 1.1- and 1.2. Therefore I determined the of JBIR-19 to treat the gene-deletion strains pooled culture is 2.5-5 μ M.

I treated pooled gene-deletion strains with or without indicated concentrations of JBIR-19 (Table 1). Experimental procedure is described as Figure 6. Briefly, to effectively detect difference of relative abundance in pooled culture, homozygous deletion pools were cultured for seven generations, and heterozygous deletion pools were cultured for 18 generations. The heterozygous strains were grown for a longer period, since heterozygous phenotypes tend to be more subtle than homozygous phenotypes (Pierce *et al.*, 2007). I extracted genomic DNA from each culture, and mixed the DNA of homozygous and heterozygous pool with the same concentrations of JBIR at the ratio of 4:1 of DNA concentration in order to approximately adjust average copy number of DNA per strain in both pools. Barcode sequences were amplified from extracted genomic DNA and labeled with fluorescently-labeled common primers. Amplified barcodes labeled with different fluorescence colors were mixed, and relative abundance of amplified barcodes was detected by hybridization of amplified tags to a custom oligonucleotide array carrying the barcode complements. To determine relative strain sensitivity, the barcode array data was analyzed with Feature Extraction Ver. 9.5. This software automatically calculates log ratio of barcode signal processed intensity between with JBIR-19 treatment and without JBIR-19 treatment, and p-value of log ratio.

I detected the gene-deletion strains, which indicated slower growth in the

presence of 2.5 and 5 μ M JBIR-19 than that in the absence of JBIR-19 by 6 barcode array experiments from 2 independent cultures (Table1). The greater log ratio is higher sensitive to JBIR-19. As a result, Homozygous deletion of *YLR111W*, *DHH1*, *CCW12* and *SNF5* and heterozygous deletion of *SPC98*, *PAB1* and *RSC9* showed p-value < 0.01 for all 6 features (that is replicates for detecting one strain in an array) in all 6 array experiments, indicating reproducible growth retardation in the presence of JBIR-19 (Figure 7). In addition, these 7 strains showed greater log ratio than the other strains. It is indicated that these 7 strains appeared to be specifically sensitive to JBIR-19.

JBIR-19 sensitivity in independent culture

To confirm the result of the competitive growth assay, cells of seven deletion strains were separately grown in YPD liquid media in the presence of JBIR-19 at 25°C (Figure 8A). Doubling time was calculated by exponential approximation with data points of OD₆₀₀, and relative growth rate was calculated. The greater relative growth rate means higher sensitive to JBIR-19. As shown Figure 8A, $\Delta dhh1$ showed more significantly sensitive to JBIR-19 than the other strains. In addition, $\Delta dhh1$ showed sensitivity to JBIR-19 in a concentration-dependent manner, suggesting that $\Delta dhh1$ was specifically sensitive to JBIR-19. Other strains showing JBIR-19 sensitivity in a competitive growth assay did not show striking concentration-dependent growth retardation in the presence of JBIR-19. For example, haploid $\Delta snf5$ (Figure 8A), $\Delta pab1$ / *PAB1* and $\Delta spc98$ / *SPC98* (Figure 8B) was showed the same sensitivity to JBIR-19 as wild-type strain. From these results, I focused on $\Delta dhh1$ for further analysis.

Morphology of bleomycin treated cells and G1/S cyclin transcription in JBIR-19 treated cells

The *DHH1* gene encodes a DEAD-box RNA helicase that may have a role in mRNA transport and translation (Coller *et al.*, 2001). *DHH1* also have an essential role for G1/S DNA-damage checkpoint recovery in *S. cerevisiae*. The peak of *CLN2* (G1/S cyclin) mRNA accumulation is delayed in the $\Delta dhh1$ cells compared to the wild-type after UV treatment (Bergkessel *et al.*, 2004). In addition, Chemical genomic assays revealed that homozygous deletion of *DHH1* is significantly sensitive to DNA damaging agent bleomycin (1.13 $\mu\text{g/ml}$) (Hillenmeyer *et al.*, 2008). Based on the above information, it is suggested that the effect of JBIR-19 and DNA damaging condition is similar. If this hypothesis is correct, bleomycin-treated cells will have elongated cell morphology like JBIR-19 treated cells and contrary, JBIR-19-treated cells will show delayed *CLN2* mRNA accumulation. To test this hypothesis, I observed the effect of bleomycin on cell morphology and effect of JBIR-19 on *CLN2* mRNA accumulation.

First I determined the concentration of bleomycin for morphology observation. The cells of wild-type and $\Delta dhh1$ were grown in the presence of indicated concentration of bleomycin (Figure 9) and growth was monitored at OD600. Doubling time was calculated and rate of growth inhibition was calculated. I decided to observe cell morphology in diploid wild-type cells and $\Delta dhh1$ cells with 50% of growth inhibition (IC_{50}) of bleomycin (Table 2).

In order to test whether bleomycin induced elongated bud morphology like

JBIR-19, cell morphology of wild-type and $\Delta dhh1$ cells in the presence of JBIR-19 or bleomycin was observed with phase-contrast microscope (Figure 10). JBIR-19 induced elongated bud morphology in wild-type diploid cells, consistent with Kozone *et al.*, 2009 (Figure 10A). JBIR-19 induced remarkable elongated bud morphology in $\Delta dhh1$ cells although $\Delta dhh1$ cells had a slightly elongated bud in the absence of JBIR-19. Similarly, bleomycin induces elongated bud morphology both in wild-type and $\Delta dhh1$ cells, although the effect is not so obvious as in the case of JBIR-19. These results suggested bleomycin and JBIR-19 induced elongated bud morphology and the effect of JBIR-19 and DNA damaging condition were similar.

To further verify the hypothesis as described above, I investigated effect of JBIR-19 on *CLN2* mRNA accumulation. Cells of wild-type or $\Delta dhh1$ strain were treated with alpha-factor for 2 h to arrest at G1, and then released to fresh medium in the presence or absence of JBIR-19. After incubation at indicated time, cells were collected and amount of *CLN2* mRNA was tested by Northern blotting (Figure 11). In the absence of JBIR-19, the peak of *CLN2* expression was delayed 15~30 min in the $\Delta dhh1$ strain compared to wild-type strain. However, in the presence of JBIR-19, the peak of *CLN2* mRNA was delayed 30~45 min in the $\Delta dhh1$ cells compared to Δ wild-type cells. This result suggested JBIR-19 induce the G1/S transition delay in $\Delta dhh1$ strain.

Discussion

I attempted to identify the cellular targets of novel compound JBIR-19 isolated with morphology-based assay of *S.cerevisiae* to understand the cellular mode of action. For this purpose, I employed a method to comprehensively survey fitness of yeast deletion mutants using a competitive growth assay. I screened JBIR-19 sensitive mutants from homozygous deletion strains and heterozygous deletion strains. In screening homozygous deletion strains, synthetic lethality data can aid in interpreting the results (Parsons, *et al.*, 2004). Homozygous deletions corresponding to synthetic lethal partners of the drug target should be more sensitive to the drug, because the drug mimics a deletion (or partial deletion) of the drug target (Figure 4C). Homozygous deletion strains can also be used to identify the target protein encoded by gene resistant to a compound (Figure 4B, Pierce, *et al.*, 2007). Screening heterozygous deletion strains can be used for the purpose of identifying novel targets of a compound, based on 'Drug-induced haploinsufficiency' (Figure 4A, Giaever, *et al.*, 2004, Giaever *et al.*, 1999, Lum *et al.*, 2004).

The results indicated that JBIR-19 specifically inhibits growth of homozygous $\Delta dhh1$ deletion mutants. As discussed above, this interprets that JBIR-19 target is a *DHH1* product itself, or the products of synthetic lethal with *DHH1* (Figure 4B and 4C). I think that the former possibility is unlikely for following reason. If the target of JBIR-19 was the *DHH1* product, wild-type cells grown in the presence of JBIR-19 would show resistance. However, wild-type cells showed a little sensitivity to the compound (Figure 9). Thus, it is likely that JBIR-19 target is the products of

synthetic lethal with *DHH1*.

I found that JBIR-19 treatment resulted in delay of *CLN2* mRNA accumulation in $\Delta dhh1$ deletion mutant. I also observed that bleomycin, inducing specific sensitivity in $\Delta dhh1$ deletion mutant, forms elongated cell morphology like as JBIR-19 treated cell. These results suggest that JBIR-19 may induce the delay of G1/S cyclin accumulation by inhibiting the products responsible for the G1/S progression in recovery from DNA damage response process and thus induce growth retardation (Figure 12, lower right). In combination with competitive growth assay, the target of JBIR-19 would have following features. 1, It shows synthetic lethal with *DHH1*: 2, It involves in G1/S progression: 3, Its deletion results in elongated cell morphology.

Several genes that are synthetic lethal with *DHH1* have been reported and that are required for bud formation. For example, *ELM1* is included as the gene responsible for bud formation. *ELM1* codes serine/threonine kinase regulating cellular morphology (Garrett et al., 1997). Mutation in *ELM1* induced elongation of cells and double mutation of *DHH1* and *ELM1* showed abnormal cell morphology (Moriya et al., 1999). In addition, bud axis ratio of 4718 haploid mutants was quantified with Calmorph and that of $\Delta elm1$ was 1.221, ranked 13th in 137 mutants having significantly elongated bud morphology (Watanabe et al., 2009). Elm1p kinase activity is not only responsible for bud formation, but also for the activity during early G1 phase. Inhibition of Elm1p kinase activity during early G1 causes defects in the organization of septins, and inhibition of Elm1p kinase activity in a strain lacking the redundant G1 cyclins *CLN1* and *CLN2* is lethal (Sreenivasan et al., 2003).

SSD1, synthetic lethal with *DHH1*, is also included as the gene related for cell morphology and cell progression from G1 to S phase. Three mutations of *DHH1*,

ELM1 and *SSD1* showed abnormal cell morphology (Moriya *et al.*, 1999). In addition, *SSD1* is identified as a polymorphic gene, that in some versions can suppress the lethality due to a deletion of *SIT4* which is required late G1 progression for S phase. Those result revealed that *SSD1* protein is implicated in G1 control (Sutton *et al.*, 1991).

Elm1p and Ssd1p related for bud formation and G1/S transition are thought to be JBIR-19 target candidates. JBIR-19 possibly perturbs the function of these proteins and induces growth retardation due to the delay of G1/S transition and elongated bud morphology in $\Delta dhh1$ cells. To ensure that whether these proteins is target of JBIR-19 or not, it is necessary that further investigation for the phenotype such as growth in gene-deletion mutants of *ELM1* or *SSD1* with JBIR-19 treatment.

A compendium of chemical-genetic assay that is a collection of fitness profile of mutants in the presence of various compounds enables to predict target of compounds based on similarity of profiles (Parsons *et al.*, 2004). Comparing the profile of JBIR-19 and that of DNA damage condition, it can be clear that the reason why $\Delta dhh1$ is specifically sensitive to JBIR-19. In addition, if their profiles are similar, JBIR-19 is proved out to be DNA damaging agent and the result leads to development of the new drug.

Materials and Methods

Yeast strains and growth condition

A *Saccharomyces cerevisiae* heterozygous essential gene-deletion strain collection and a homozygous non-essential gene-deletion strain collection established by the *Saccharomyces* Genome Deletion Project (SGDP) were purchased from OPEN BIOSYSTEMS (OPEN BIOSYSTEMS, USA). Haploid non-essential gene-deletion strain collection, a wild-type diploid strain (BY4743) and wild-type haploid strain ($\Delta his3$) were purchased from EUROSCARF (Germany). *S. cerevisiae* was grown in the rich yeast medium (YPD). YPD medium contained 1% (w/v) bacto yeast extract (BD BIOSCIENCE, USA), 2% (w/v) bacto peptone (BD BIOSCIENCE) and 2% (w/v) dextrose.

Construction of deletion pool

The collection of heterozygous deletion strains and homozygous deletion strain were supplied as saturated glycerol stocks in 96-well plates. Heterozygous deletion strains were transferred to YPD supplemented with Geneticin (200 $\mu\text{g}/\text{ml}$, as G-418 from WAKO, Japan) agar plates with RoToR High-density Arrayer (SINGER INSTRUMENTS, UK). Homozygous deletion strains were inoculated to the plates with two 48-well pinholders instead of RoToR. Cells were grown for 72 hours at 30°C. Colonies were formed until they reached to approximately equal abundance. Cells was

soaked off the plates with a spreader by adding 5 ml of YPD liquid media supplemented with Geneticin (200 µg/ml) to each plate and agitating the plate to resuspend the cells. After the cells were resuspended, liquid were pooled in a 50 ml centrifuge tube or a flask by transferring 2.4 ml from each plate with a pipette. Cells were diluted by YPD liquid media supplemented with Geneticin (200 µg/ml) to adjust to a final concentration of 1.1×10^9 cells/ml and glycerol was added to final concentration of 15%. The pool were mixed well and aliquot into individually capped 0.5 ml PCR tubes with 25, 100, 250 µl of pool, and stored at -80°C until before use. The collection of 1133 heterozygous deletion strains and 4548 homozygous deletion strain were pooled, respectively.

Drugs

JBIR-19 was provided by Dr. K. Shinya (AIST). Bleomycin was purchased from SIGMA (USA). JBIR-19 was dissolved with dimethylsulphoxide (DMSO). Synthetic oligonucleotides were purchased from GREiNER,(Japan). 0.1% DMSO was used as a negative control. Bleomycin was dissolved with sterilized water.

Determination of JBIR-19 concentration to treat the pooled culture

Wild-type diploid cells were pre-cultured, diluted to 4 ml YPD to adjust to a final concentration of 5.5×10^5 cells/ml, and were grown at 30°C with or without

JBIR-19 at different concentrations which were 3 serial dilutions of 2-fold from 10 μM . OD_{600} was measured for every 10 minutes by biophotorecorder (TVS062CA, ADVANTEC, Japan) and averaged within 5-continuous data-points moving average window. Doubling time was then calculated by exponential approximation with 20 continuous data points at R^2 between OD_{600} of and culture time > 0.995 . Growth inhibition rate was calculated as (doubling time in the presence of JBIR-19/doubling time in the absence of JBIR-19).

JBIR-19 treatments of pooled culture

The heterozygous deletion strain pool and homozygous deletion strain pool were diluted to 4 ml YPD to adjust to a final concentration of 1.4×10^5 and 5.5×10^5 cells/ml, respectively. The cells were grown with or without JBIR-19. Heterozygous deletion strain pool was grown for 18 generations and homozygous deletion strain pool was grown for 7 generations. The culture of 1 ml was collected to each aliquot and stored at -80°C .

Genomic DNA isolation, quantification and normalization

Genomic DNA was subsequently isolated using the MasterPureTM-Yeast DNA purification kit (EPICENTRE, USA) and quantified. Genomic DNA of heterozygous deletion strains and homozygous deletion strains were mixed with one to four and reached to final concentration of 20 ng/ μl . The genomic DNA was stored at -20°C .

Tag Amplification

The barcode sequences were amplified from and Cy3- or Cy5-labeled from genomic DNA isolated from cultures for following procedures. The UP tag and DOWN tag barcodes were amplified and labeled in separate 50 μ l reactions with 5 μ l (100 ng) of genomic DNA, 2.5 μ l of UP tag or DOWN tag primer mix, 25 μ l of 2 \times Extaq pre-mix (TAKARA, Japan), and 17.5 μ l of sterilized water. The UP tag primer mix contained 5 μ M of unlabeled UP tag forward primer (5'-gatgtccacgaggtctct-3') and 50 μ M of Cy3- or Cy5-labeled reverse UP tag primer (5'-Cy-gtcgactgcagcgtacg-3'). The DOWN tag primer mix contained 5 μ M of unlabeled DOWN tag reverse primer (5'-cgggtgcggtctcgtag-3') and 50 μ M of Cy3- or Cy5-labeled forward DOWN tag primer (5'-Cy-cgagctcgaattcatcg-3'). PCR conditions were as follows; 2 min at 94°C; then 50 cycles of 10 sec at 94°C; 10 sec at 50°C; 20 sec at 72°C; hold at 4°C. PCR products were stored at -80°C.

Hybridization to Tag Array

Labeled tags were hybridized to custom-ordered oligonucleotide microarrays (AGILENT TECHNOLOGIES, USA). These arrays are consisted of 20-mer probes that were complement to barcode sequences. Hybridizations were done in 110 μ l with 20 μ l of Cy5-labeled tags mixture, 20 μ l of Cy3-labeled tags mixture, 2 μ l UP tag blocking mix, 2 μ l DOWN tag blocking mix, and 66 μ l of Hybridization Buffer mix (AGILENT TECHNOLOGY) for 4 hours at 42°C. UP tag blocking mix contained 500 μ M of unlabeled UP tag primer described above and 500 μ M of U2RC primer

(5'-cgtacgctgcaggtcgac-3'). DOWN tag blocking mix contained 500 μ M of unlabeled DOWN tag primer described above and 500 μ M of D2RC primer (5'-atcgatgaattcgagctcg-3'). Hybridization Buffer mix contained 2 \times GE Hi-RPM Hybridization Buffer and 10 \times blocking agent with five to one (v/v) (AGILENT TECHNOLOGIES). Arrays were washed in Gene Expression Wash Buffer containing 0.005% Triton X-102 (AGILENT TECHNOLOGIES). Slides were then scanned on G2565BA microarray scanner (AGILENT TECHNOLOGIES). Array quantification was done with Feature Extraction Ver 9.5(AGILENT TECHNOLOGIES).

The confirmation of the compound growth inhibition effect

Culture of wild-type cells or mutant cells was diluted to 1.5×10^4 cells/ml. Diluted culture (20 μ l) was dispensed to each well of 96-well microplate. Eighty μ l YPD medium which contained 3.2 or 6.3 μ M JBIR-19 was added to each well to produce to the final concentration of 2.5 or 5 μ M in 100 μ l culture. Culture was incubated for 23 hours at 25°C.

I tested for the growth inhibition to wild-type by adding bleomycin at different concentrations which were 6 serial dilution of 2-fold from 2 μ g/ml and for that to $\Delta dhh1$ by adding the treatment at different concentrations which were 10 serial dilutions of 2-fold from 200 ng/ml. Culture of wild-type and $\Delta dhh1$ was incubated for 25 hours and 39 hours, respectively.

OD₆₀₀ was measured with plate-reader (SPECTRAmax, MOLECULAR DEVICES, USA). Doubling time and relative growth rate was calculated same as the determination of the concentration of JBIR-19. IC₅₀ was defined as the concentration

which indicated relative growth inhibition rate = 2.

Phase-contrast image analysis

1.5×10^5 cells/ml of diploid wild-type cells and $\Delta dhh1$ cells were grown with or without the treatment (JBIR-19 or bleomycin) for 24 hours at 25°C. Yeast cells were observed the cell morphology with a AxioImager M1 (CARL ZEISS, Germany) and Plan Apochromat 100x objective. Images were captured using a cooled CCD camera CoolSNAPHQ (ROPER SCIENTIFIC PHOTOMETRICS, USA) interfaced with AxioVison (CARL ZEISS).

Synchronization of cells with α -factor

Eighty ml of cells in YPD medium was grown to 1.0×10^7 cells/ml at 25°C and was synchronized in G1 phase with 5 $\mu\text{g/ml}$ of α -factor (SIGMA) treatment for 2 hours. The α -factor was then removed by washing twice with YPD medium. The cells were released to fresh 40 ml YPD media with or without 2.5 μM JBIR-19. After releasing, 5 ml of samples were collected every 15 minutes and stored at -80°C.

RNA Extraction and Northern Blotting

Total RNA was extracted from cells by ISOGEN according to the manufacturer's protocol (WAKO). 5 μg of total RNA samples were denatured in the

loading buffer, separated on a 0.9% agarose gel and transferred to a Biotodyne PLUS 0.45 μm membrane (PALL CORPORATION, USA). The nonradioactive probes (*CLN2* and *ACT1* digoxigenin (DIG)-labeled riboprobes) were transcribed *in vitro* using Taq polymerase with a template of DNA fragments isolated from wild-type cells. The membranes were prehybridized 1 hour at 50°C and hybridized with DIG-labeled probe overnight at 50°C. After hybridization, unhybridized probe was removed by washing in following buffers. Low stringency washes ($2\times\text{SSC}$ and 0.1% SDS) to remove the hybridization solution and unhybridized probe were done twice for 5 minutes at room temperature. High stringency washes ($0.1\times\text{SSC}$ and 0.1% SDS) to remove partially hybridized molecules were done three times for 10 minutes at 68°C. The membrane was then equilibrated for 5 minutes in buffer 1 (100 mM maleic acid and 150 mM NaCl, pH 7.5) containing 0.3% Tween-20, and blocked 60 minutes in blocking solution (buffer 1 containing 2% blocking reagent). The antibody (alkaline-phosphatase conjugated anti-DIG, ROCHE DIAGNOSTICS, USA) was diluted (1/10000) in blocking solution and the membrane was incubated for 60 minutes at room temperature. The membrane was washed three-times in buffer 1 containing 0.3% Tween-20 for 5 minutes at room temperature and equilibrated for 5 minutes in detection buffer (3 M Tris-HCl pH 9.5, 2 M NaCl and 2 M MgCl_2). Detection was performed with a few drops of CPD-Star chemiluminescent substrate solution and incubated for 5 minutes at room temperature in the dark. Bands were detected by the LAS-1000 plus luminescent image analyzer (FUJI-PHOTO FILM, Japan).

References

BERGKESSEL, M. & REESE, J. 2004. An essential role for the *Saccharomyces cerevisiae* DEAD-box helicase DHH1 in G1/S DNA-damage checkpoint recovery. *Genetics*, 167, 21-33.

COLLER, J., TUCKER, M., SHETH, U., VALENCIA-SANCHEZ, M. & PARKER, R. 2001. The DEAD box helicase, Dhh1p, functions in mRNA decapping and interacts with both the decapping and deadenylase complexes. *RNA*, 7, 1717-27.

GARRETT, J. 1997. The control of morphogenesis in *Saccharomyces cerevisiae* by Elm1 kinase is responsive to RAS/cAMP pathway activity and tryptophan availability. *Mol Microbiol*, 26, 809-20.

GIAEVER, G. 2003. A chemical genomics approach to understanding drug action. *Trends Pharmacol Sci*, 24, 444-6.

GIAEVER, G., CHU, A., NI, L., CONNELLY, C., RILES, L., VRONNEAU, S., DOW, S., LUCAU-DANILA, A., ANDERSON, K., ANDR, B., ARKIN, A., ASTROMOFF, A., EL-BAKKOURY, M., BANGHAM, R., BENITO, R., BRACHAT, S., CAMPANARO, S., CURTISS, M., DAVIS, K., DEUTSCHBAUER, A., ENTIAN, K., FLAHERTY, P., FOURY, F., GARFINKEL, D., GERSTEIN, M., GOTTE, D., GLDENER, U., HEGEMANN, J., HEMPEL, S., HERMAN, Z., JARAMILLO, D., KELLY, D., KELLY, S., KETTER, P., LABONTE, D., LAMB, D., LAN, N., LIANG,

H., LIAO, H., LIU, L., LUO, C., LUSSIER, M., MAO, R., MENARD, P., OOI, S., REVUELTA, J., ROBERTS, C., ROSE, M., ROSS-MACDONALD, P., SCHERENS, B., SCHIMMACK, G., SHAFER, B., SHOEMAKER, D., SOOKHAI-MAHADEO, S., STORMS, R., STRATHERN, J., VALLE, G., VOET, M., VOLCKAERT, G., WANG, C., WARD, T., WILHELMY, J., WINZELER, E., YANG, Y., YEN, G., YOUNGMAN, E., YU, K., BUSSEY, H., BOEKE, J., SNYDER, M., PHILIPPSEN, P., DAVIS, R. & JOHNSTON, M. 2002. Functional profiling of the *Saccharomyces cerevisiae* genome. *Nature*, 418, 387-91.

GIAEVER, G., FLAHERTY, P., KUMM, J., PROCTOR, M., NISLOW, C., JARAMILLO, D., CHU, A., JORDAN, M., ARKIN, A. & DAVIS, R. 2004. Chemogenomic profiling: identifying the functional interactions of small molecules in yeast. *Proc Natl Acad Sci U S A*, 101, 793-8.

GIAEVER, G., SHOEMAKER, D., JONES, T., LIANG, H., WINZELER, E., ASTROMOFF, A. & DAVIS, R. 1999. Genomic profiling of drug sensitivities via induced haploinsufficiency. *Nat Genet*, 21, 278-83.

HARDING, M., GALAT, A., UEHLING, D. & SCHREIBER, S. 1989. A receptor for the immunosuppressant FK506 is a cis-trans peptidyl-prolyl isomerase. *Nature*, 341, 758-60.

HILLENMEYER, M., FUNG, E., WILDENHAIN, J., PIERCE, S., HOON, S., LEE, W., PROCTOR, M., ST ONGE, R., TYERS, M., KOLLER, D., ALTMAN, R., DAVIS, R.,

NISLOW, C. & GIAEVER, G. 2008. The chemical genomic portrait of yeast: uncovering a phenotype for all genes. *Science*, 320, 362-5.

HOON, S., ST ONGE, R., GIAEVER, G. & NISLOW, C. 2008. Yeast chemical genomics and drug discovery: an update. *Trends Pharmacol Sci*, 29, 499-504.

KOZONE, I., UEDA, J., WATANABE, M., NOGAMI, S., NAGAI, A., INABA, S., OHYA, Y., TAKAGI, M. & SHIN-YA, K. 2009. Novel 24-membered macrolides, JBIR-19 and -20 isolated from *Metarhizium* sp. fE61. *J Antibiot (Tokyo)*, 62, 159-62.

LEE, W., ST ONGE, R., PROCTOR, M., FLAHERTY, P., JORDAN, M., ARKIN, A., DAVIS, R., NISLOW, C. & GIAEVER, G. 2005. Genome-wide requirements for resistance to functionally distinct DNA-damaging agents. *PLoS Genet*, 1, e24.

LUM, P., ARMOUR, C., STEPANIANTS, S., CAVET, G., WOLF, M., BUTLER, J., HINSHAW, J., GARNIER, P., PRESTWICH, G., LEONARDSON, A., GARRETT-ENGELE, P., RUSH, C., BARD, M., SCHIMMACK, G., PHILLIPS, J., ROBERTS, C. & SHOEMAKER, D. 2004. Discovering modes of action for therapeutic compounds using a genome-wide screen of yeast heterozygotes. *Cell*, 116, 121-37.

MORIYA, H. & ISONO, K. 1999. Analysis of genetic interactions between DHH1, SSD1 and ELM1 indicates their involvement in cellular morphology determination in *Saccharomyces cerevisiae*. *Yeast*, 15, 481-96.

OHYA, Y., SESE, J., YUKAWA, M., SANO, F., NAKATANI, Y., SAITO, T., SAKA, A., FUKUDA, T., ISHIHARA, S., OKA, S., SUZUKI, G., WATANABE, M., HIRATA, A., OHTANI, M., SAWAI, H., FRAYSSE, N., LATG, J., FRANOIS, J., AEBI, M., TANAKA, S., MURAMATSU, S., ARAKI, H., SONOIKE, K., NOGAMI, S. & MORISHITA, S. 2005. High-dimensional and large-scale phenotyping of yeast mutants. *Proc Natl Acad Sci U S A*, 102, 19015-20.

PARSONS, A., BROST, R., DING, H., LI, Z., ZHANG, C., SHEIKH, B., BROWN, G., KANE, P., HUGHES, T. & BOONE, C. 2004. Integration of chemical-genetic and genetic interaction data links bioactive compounds to cellular target pathways. *Nat Biotechnol*, 22, 62-9.

PIERCE, S., DAVIS, R., NISLOW, C. & GIAEVER, G. 2007. Genome-wide analysis of barcoded *Saccharomyces cerevisiae* gene-deletion mutants in pooled cultures. *Nat Protoc*, 2, 2958-74.

RINE, J., HANSEN, W., HARDEMAN, E. & DAVIS, R. 1983. Targeted selection of recombinant clones through gene dosage effects. *Proc Natl Acad Sci U S A*, 80, 6750-4.

SREENIVASAN, A., BISHOP, A., SHOKAT, K. & KELLOGG, D. 2003. Specific inhibition of Elm1 kinase activity reveals functions required for early G1 events. *Mol Cell Biol*, 23, 6327-37.

SUTTON, A., IMMANUEL, D. & ARNDT, K. 1991. The SIT4 protein phosphatase

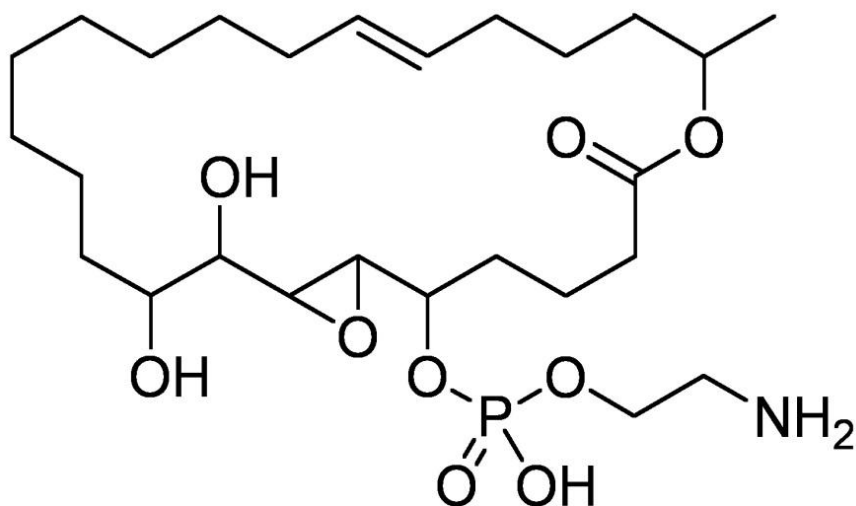
functions in late G1 for progression into S phase. *Mol Cell Biol*, 11, 2133-48.

WATANABE, M., WATANABE, D., NOGAMI, S., MORISHITA, S. & OHYA, Y. 2009. Comprehensive and quantitative analysis of yeast deletion mutants defective in apical and isotropic bud growth. *Curr Genet*, 55, 365-80.

WINZELER, E., SHOEMAKER, D., ASTROMOFF, A., LIANG, H., ANDERSON, K., ANDRE, B., BANGHAM, R., BENITO, R., BOEKE, J., BUSSEY, H., CHU, A., CONNELLY, C., DAVIS, K., DIETRICH, F., DOW, S., EL BAKKOURY, M., FOURY, F., FRIEND, S., GENTALEN, E., GIAEVER, G., HEGEMANN, J., JONES, T., LAUB, M., LIAO, H., LIEBUNDGUTH, N., LOCKHART, D., LUCAU-DANILA, A., LUSSIER, M., M'RABET, N., MENARD, P., MITTMANN, M., PAI, C., REBISCHUNG, C., REVUELTA, J., RILES, L., ROBERTS, C., ROSS-MACDONALD, P., SCHERENS, B., SNYDER, M., SOOKHAI-MAHADEO, S., STORMS, R., V/IRONNEAU, S., VOET, M., VOLCKAERT, G., WARD, T., WYSOCKI, R., YEN, G., YU, K., ZIMMERMANN, K., PHILIPPSSEN, P., JOHNSTON, M. & DAVIS, R. 1999. Functional characterization of the *S. cerevisiae* genome by gene deletion and parallel analysis. *Science*, 285, 901-6.

Figures

A



JBIR-19
from fE61

$C_{26}H_{48}NO_9P$
Exact Mass: 549.3067

B

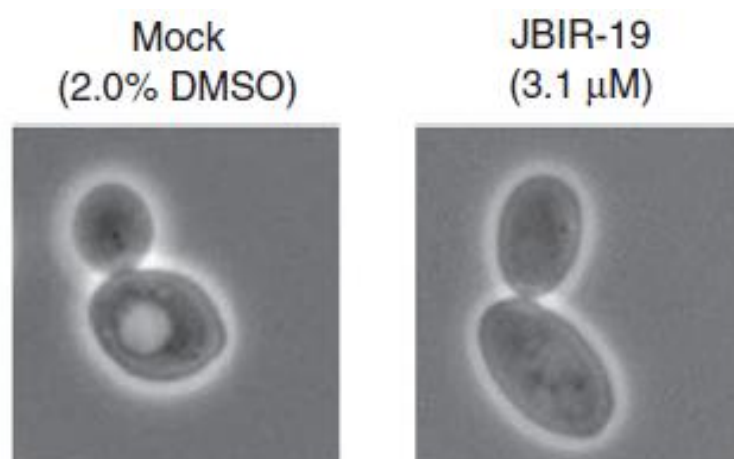


Figure 1. The structure of JBIR-19(A) and phase contrast image of diploid wild-type cells *S. cerevisiae* grown in the presence or absence of JBIR-19(B).

This Figure referred to Kozone *et al.*, 2009.



Figure 2. Deletion cassette used for constructing strains in the yeast deletion collection.

Each cassette carries the marker gene in common to each strain. The marker is flanked by two unique tag sequences, which are called the ‘uptag’ (yellow square) and the ‘downtag’ (green square). These tags were designed to be maximally distinct. The two tags flanked by four universal primer sites (colored arrows) that are common to all strains and allow the tags to be amplified from a pooled culture.

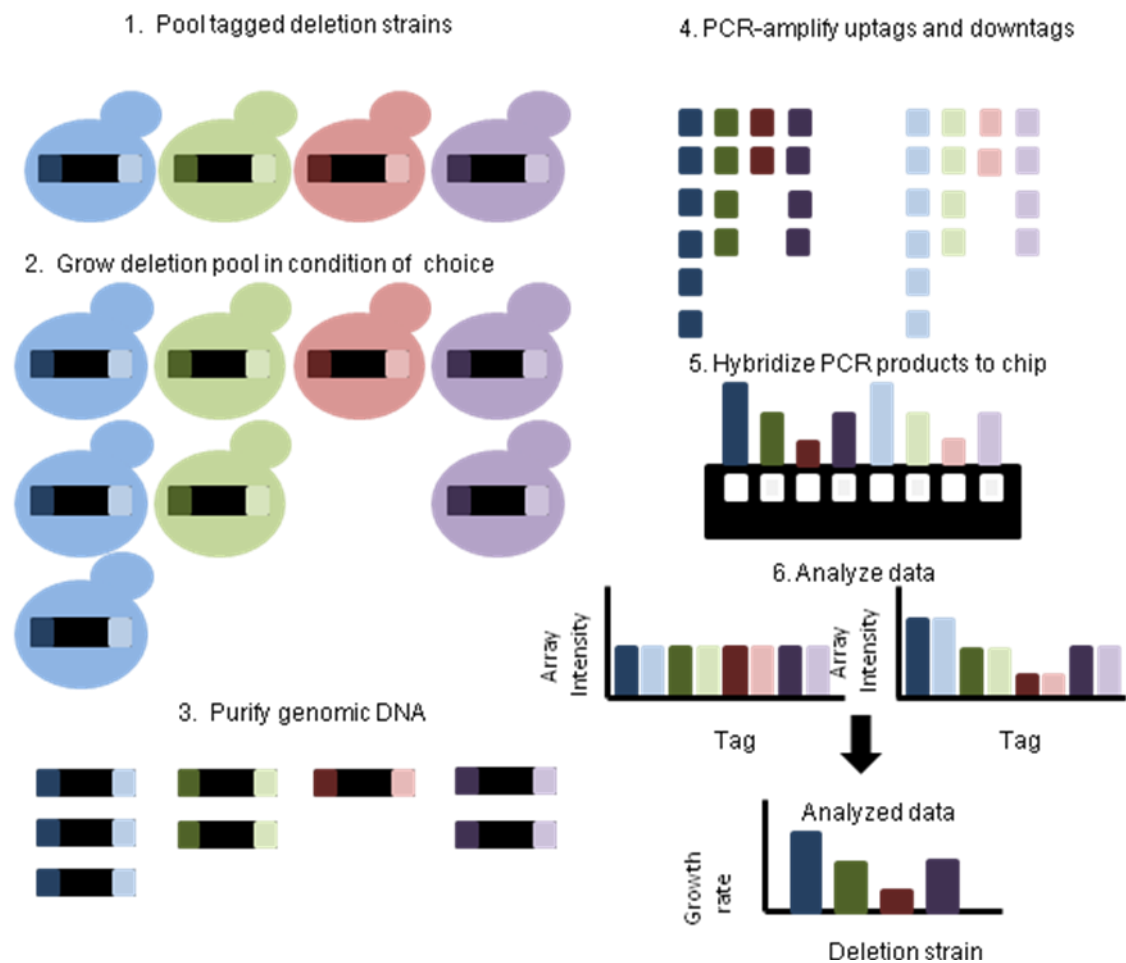


Figure 3. Outline of the competitive growth assay.

Fitness profiling of pooled deletion strains involves six main steps: (1) Strains are first pooled at approximately equal abundance. (2) The pool is grown competitively in the condition of choice. The pool of heterozygous deletion strains and the pool of homozygous deletion strains are grown separately. The strain required for growth under this condition will grow more slowly and become underrepresented in the culture (red strain). Resistant strains will grow faster and become overrepresented (blue strain). (3) Genomic DNA is isolated from cells harvested at the end of pooled growth. (4) Tags are amplified from the genomic DNA. (5) PCR products are then hybridized to a tag-array that detects tag sequence. (6) Tag intensities for the treatment sample are compared to tag intensities for a control sample to determine the relative fitness each strain. Here, the starting sample shown (1) is used as a control, (3) ~ (5) are not shown for this control sample. This figure is referred to Pierce *et al.*,2007.

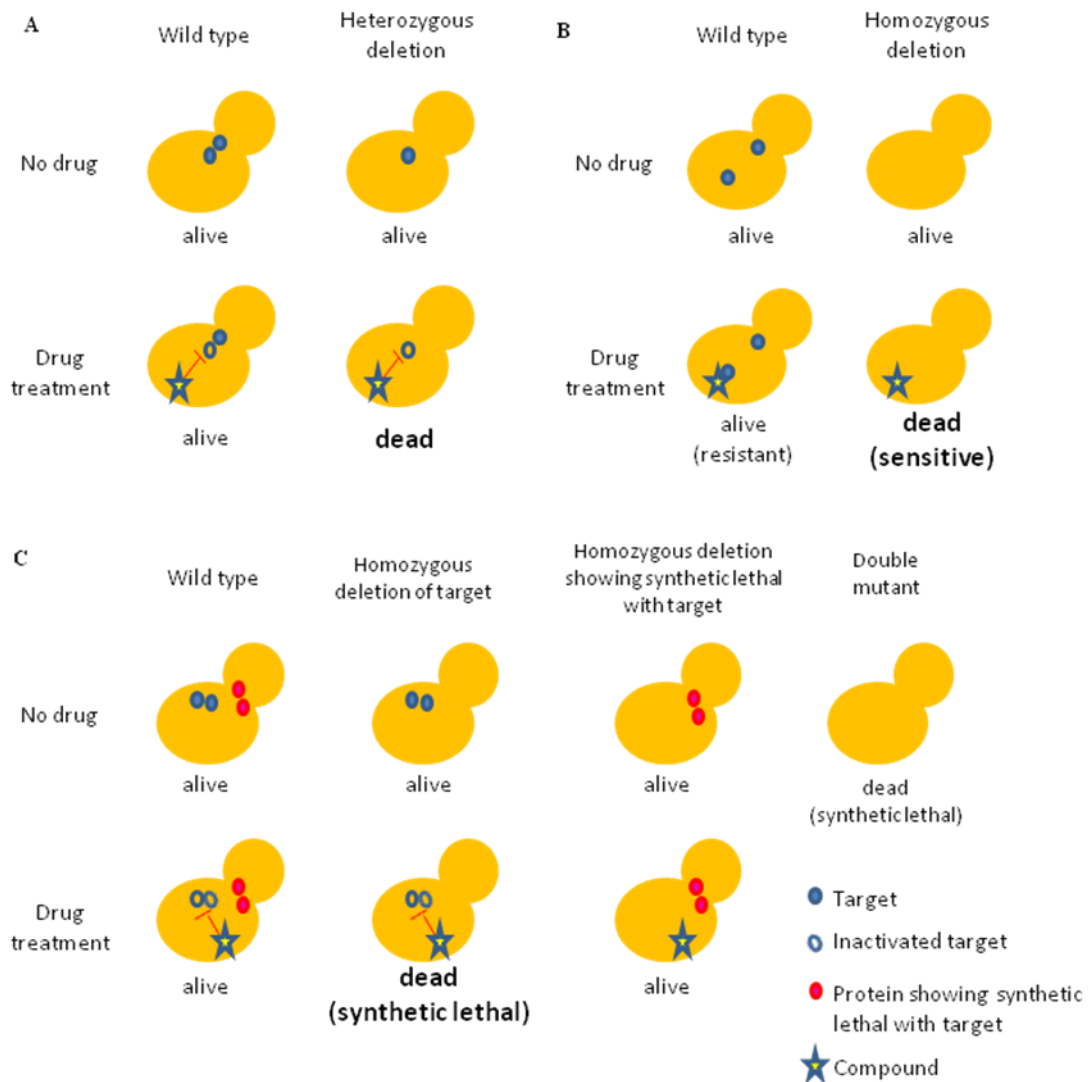
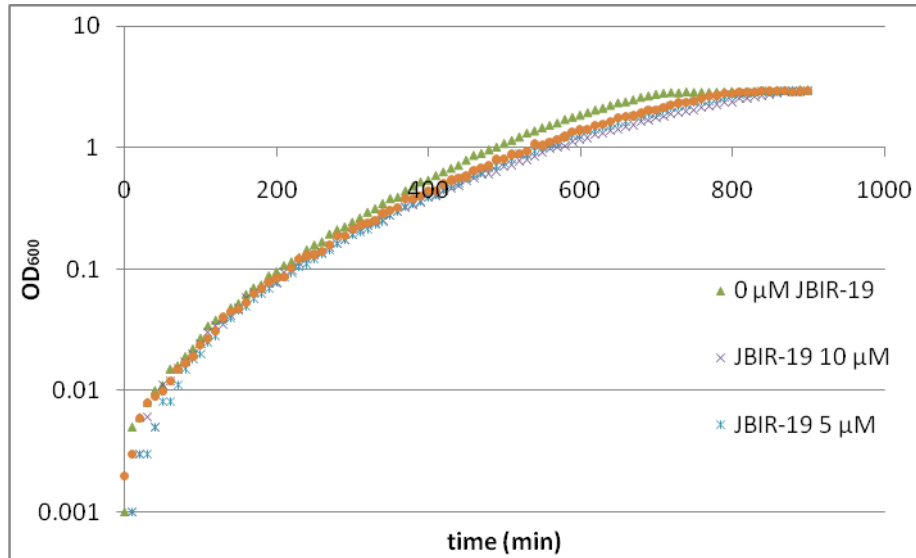


Figure 4. Possible explanation of results.

(A) Drug-induced haploinsufficiency. Reducing the copy number of a gene which codes the target (blue circles) from two to one in a diploid cell can result in sensitization to the compound of interest. Heterozygous deletion strains can be used in this strategy. (B) Drug resistance. Assuming that the target protein (blue circle) required for resistance against a drug or coping with the stress caused by a compound, deletion of the gene encoding the target protein often confers increased sensitive to the compound. Homozygous deletion strains can be used in this strategy. (C) Synthetic lethality. Synthetic lethality refer to a genetic interaction where two separate strains with viable mutations result in reduced or no growth when combined in a double mutant containing both. Extending this approach, the target can be identified with homozygous deletion strains grown in the presence of a compound. This figure is modified from Hoon *et al.*, 2008.

A



B

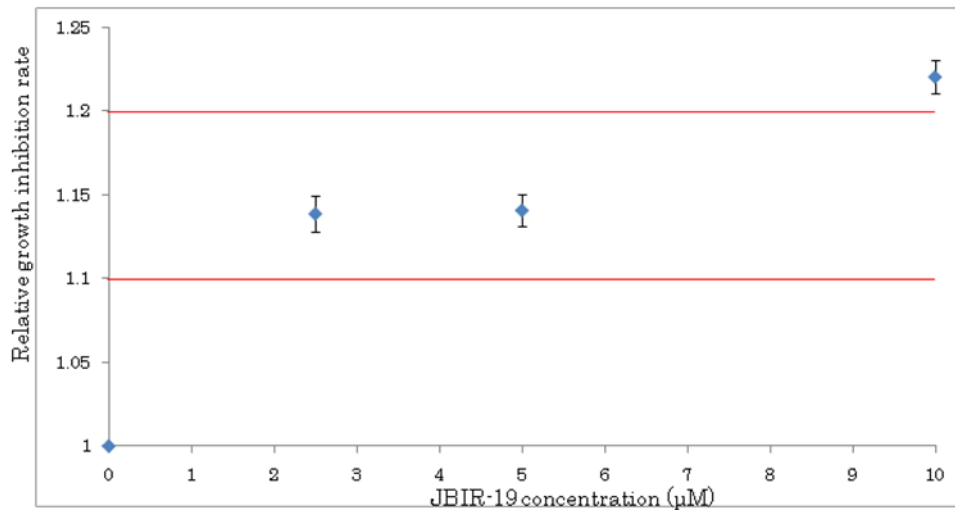


Figure 5. Growth inhibition by JBIR-19 for wild type strain.

(A) Growth in the presence or absence of JBIR-19 (B) Growth inhibition rate of JBIR-19. BY4743 was grown in YPD liquid media with or without JBIR-19 at 30°C. OD₆₀₀ was measured by biophotorecorder (ADVANTEC). The moving average of continuous 5 raw data points of OD₆₀₀ was calculated and doubling time was figured by exponential approximation with the continuous 20 average data points. Relative growth inhibition rate of JBIR-19 was calculated using the doubling time at the data points that indicated correlation factor between OD₆₀₀ and culture time more than 0.995. Relative growth inhibition rate = (doubling time at growth in the presence of JBIR-19) /

(doubling time at growth in the absence of JBIR-19).

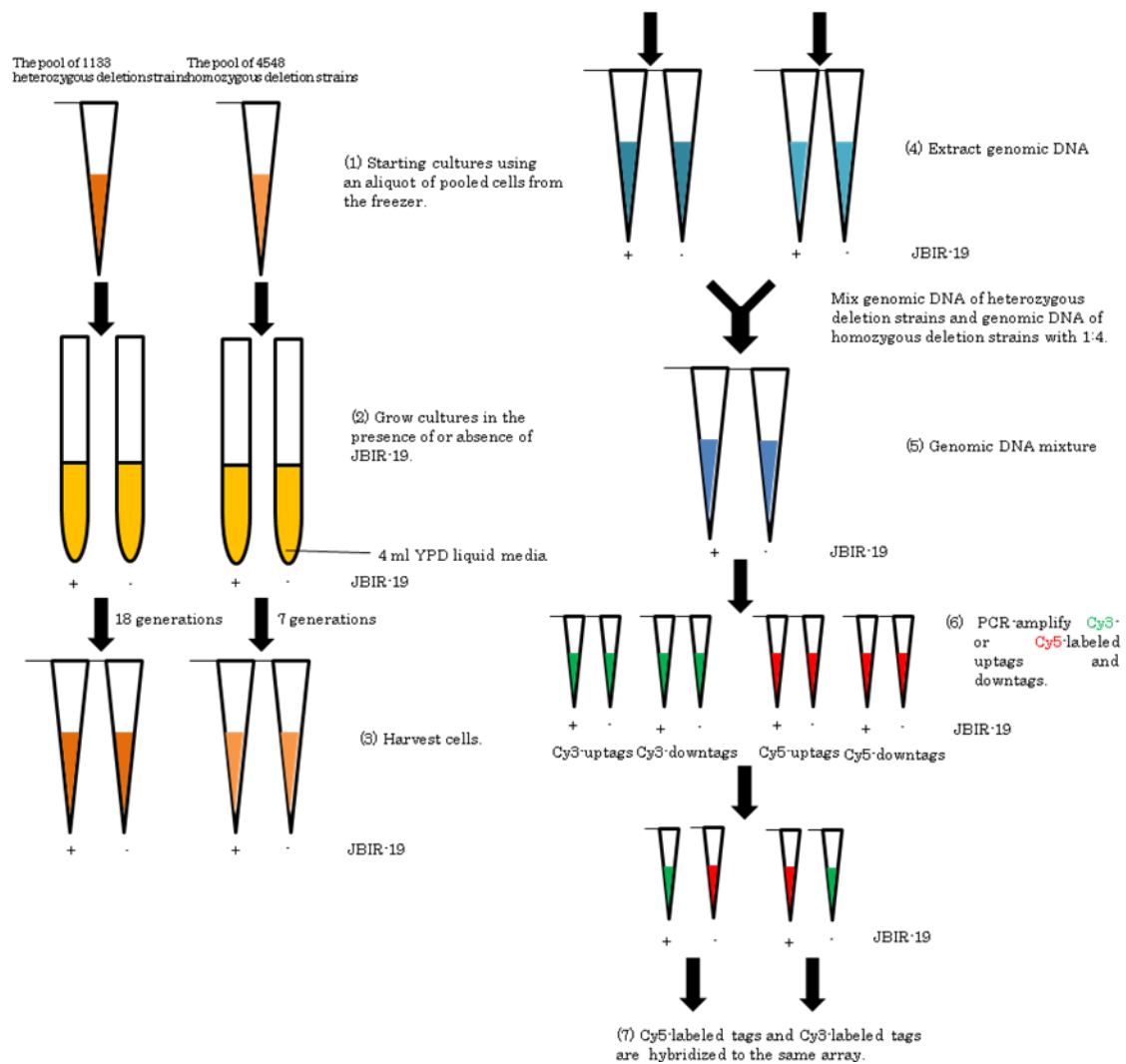


Figure 6. Outline for experimental procedure.

The pool of heterozygous deletion strain and that of homozygous deletion strains are inoculated to YPD liquid media culture separately and cells are grown for the desired number of generations. The heterozygotes are grown for a longer period, because heterozygous phenotypes tend to be more subtle than homozygous phenotypes (Pierce *et al.*, 2007). Cells are harvested by centrifugation and genomic DNA is purified from the cell pellets using a standard purification kit. Tags are PCR amplified from the purified genomic DNA. The Cy3- or Cy5-labeled uptags and downtags are amplified separately to avoid cross-reactions between the uptag and downtag primer pairs. Finally, Cy3- or Cy5-labeled tags are hybridized to a single array.

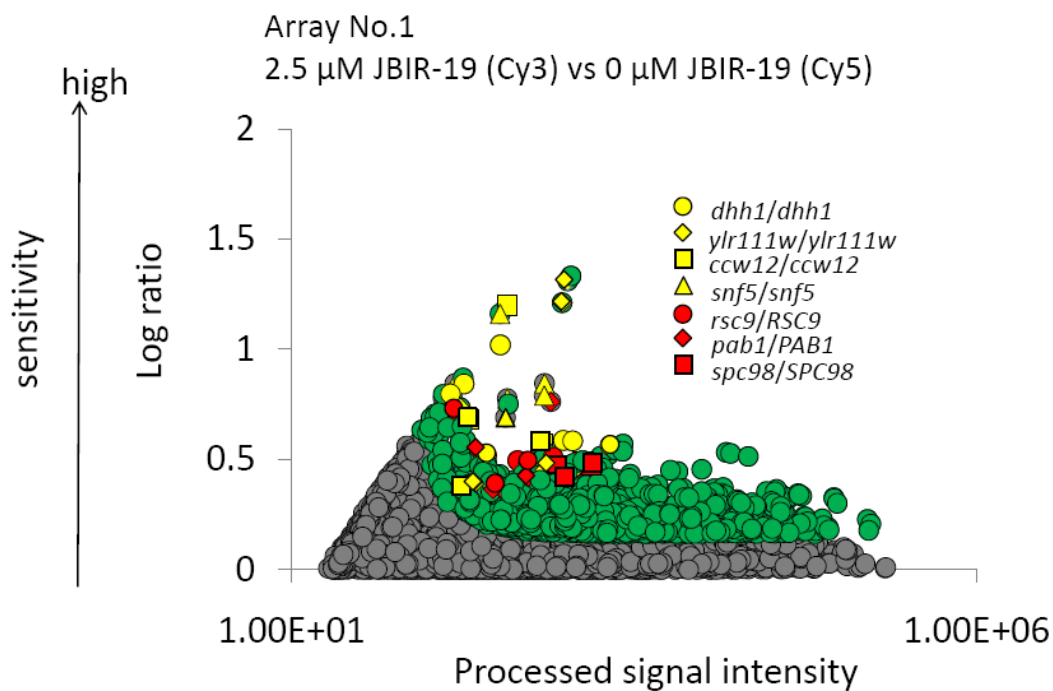
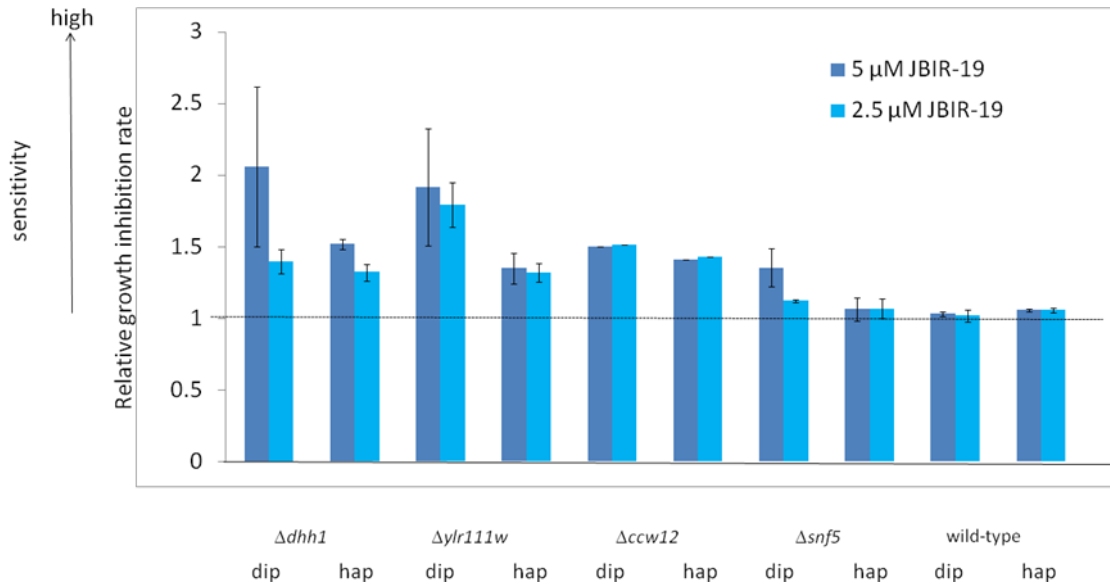


Figure 7. The deletion strains specifically sensitive to JBIR-19 with a competitive growth assay. This figure is a representative of 6 arrays from 2 independent cultures. The y axis represents the log ratio of processed signal intensity of barcode DNA between with JBIR-19 treatment and without JBIR-19 treatment. Green dots are data of each strain which meet condition of p-value < 0.01. Each array condition describes as follows: each deletion strain has up tag and down tag. 3 features for each tag are on a 44k format of custom Agilent array.

A



B

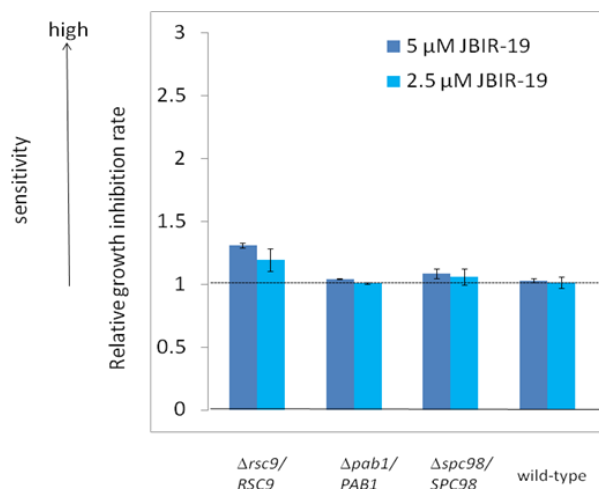


Figure 8. Deletion mutant of *DHH1* showed sensitivity to JBIR-19 in a concentration-dependent manner.

Each gene-deletion strain grown in YPD liquid media in the presence or absence of indicated concentration of JBIR-19 at 25°C. Doubling time was calculated by exponential approximation with data points of OD₆₀₀, and relative growth rate was calculated. (A) Growth inhibition rate of JBIR-19 to each homozygous diploid (dip) or haploid (hap) gene-deletion mutant. (B) Heterozygous diploid gene-deletion mutant.

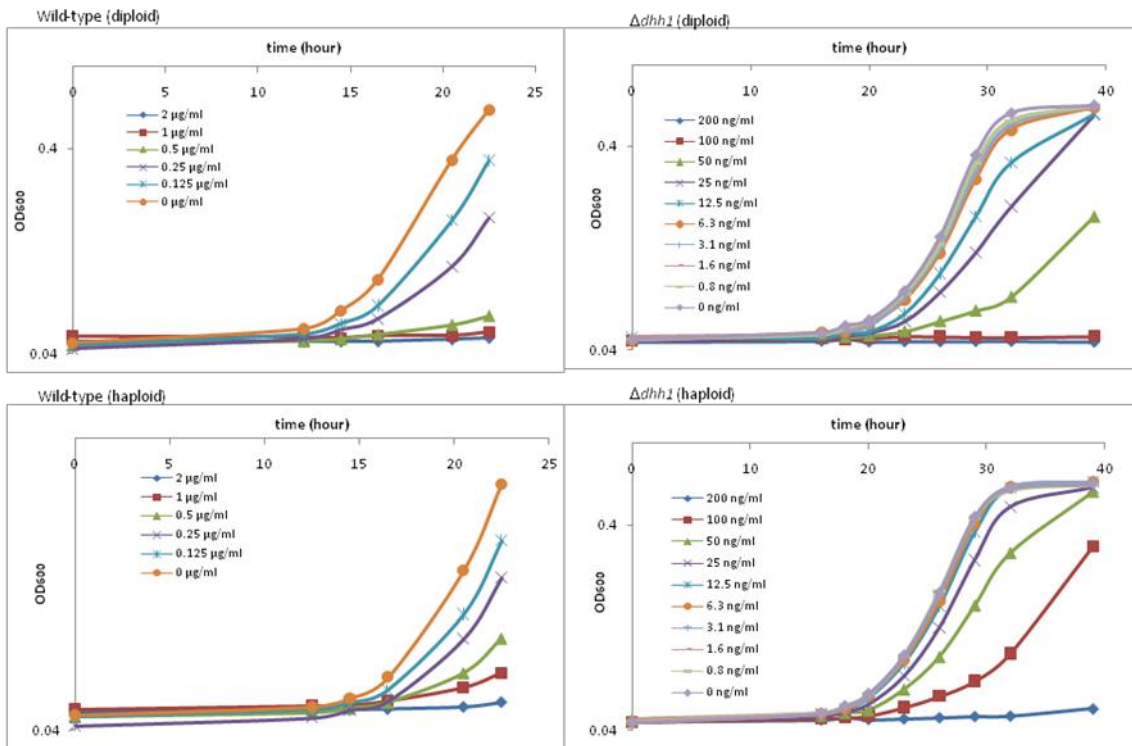
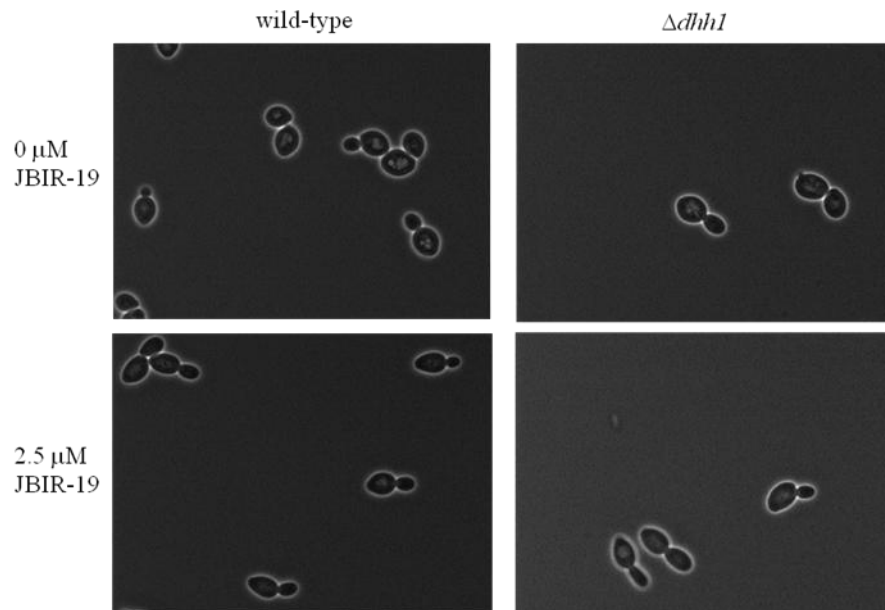


Figure 9. Deletion mutant of *DHH1* showed sensitivity to bleomycin in a concentration-dependent manner.

Wild-type or mutant strain was grown in YPD liquid media in the presence or absence of indicated bleomycin at 25°C. OD₆₀₀ in three independent culture was averaged.

A



B

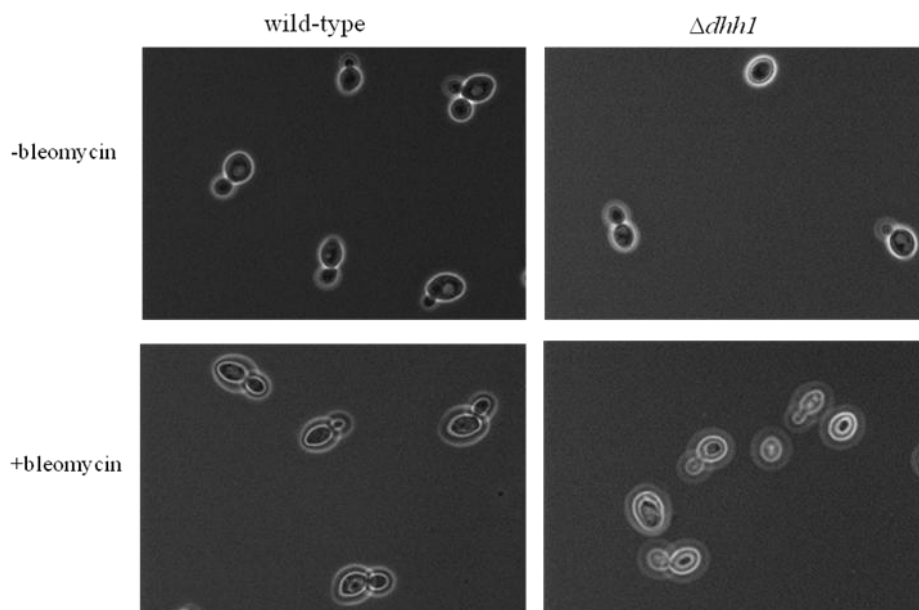


Figure 10. JBIR-19 and bleomycin induced elongated bud morphology of wild-type cells and $\Delta dhh1$ cells.

Diploid cells were grown in the presence of absence of an indicated compound for 24 hours at 25°C and observed cell morphology with phase-contrast microscope. 250 ng/ml, 25 ng/ml of bleomycin were used for wild-type cells and $\Delta dhh1$ cells, respectively.

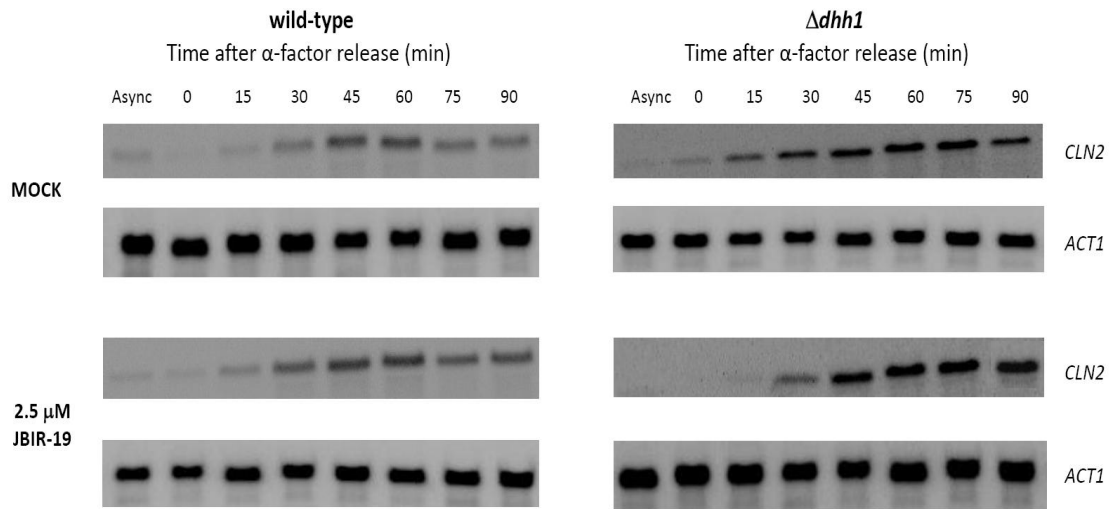


Figure 11. JBIR-19 induces the delay of *CLN2* mRNA accumulation in haploid $\Delta dhh1$ cells.

Log phase cultures grown in YPD at 25°C were synchronized in G1 by α -factor (final concentration to 5 μ g/ml) treatment for 2 hours, then the α -factor was removed, and release to fresh YPD media with or without 2.5 μ M JBIR-19. After releasing, samples were collected at every 15 min for quantifying *CLN2* mRNA by Northern blotting (5 μ g/lane of RNA extracted from each aliquots was applied). *ACT1* is a loading control.

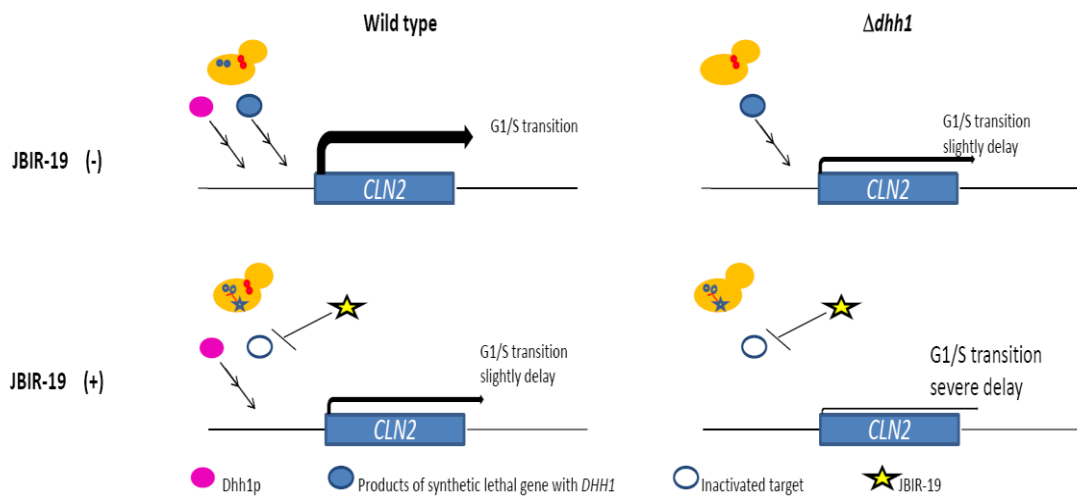


Figure 12. The G1/S transition delay induced by JBIR-19 in $\Delta dhh1$ cells.

Same symbols as **Figure. 4C** are used. Products of synthetic lethal gene with *DHH1* are thought to be candidates target of JBIR-19.

Tables

Table1. Combination of growth conditions and dyes for each array

The experiment of Array No.5 and 6 are performed previously by Dr. Nogami.

Array No.	Cy3	Cy5
1	2.5 μ M JBIR-19	0 μ M JBIR-19
2	0 μ M JBIR-19	2.5 μ M JBIR-19
3	5 μ M JBIR-19	0 μ M JBIR-19
4	0 μ M JBIR-19	5 μ M JBIR-19
5	5 μ M JBIR-19	0 μ M JBIR-19
6	0 μ M JBIR-19	5 μ M JBIR-19

Table 2. 50% inhibition concentration (IC₅₀) of bleomycin for wild-type strain and *Δdhh1*

IC₅₀ was calculated from doubling time between with and without bleomycin.

strain	IC ₅₀ (ng/ml)
wild-type (diploid)	250
wild-type (haploid)	250
<i>Δdhh1</i> (diploid)	25
<i>Δdhh1</i> (haploid)	50